The impact of chamber transparency on estimation of peatland net ecosystem exchange

Marcin Stróżecki[1,*], *Anshu* Rastogi[1], and *Radosław* Juszczak[1]

[1] Meteorology Department, Poznan University of Life Sciences, Piątkowska 94, 60-649 Poznań, Poland

Abstract. The purpose of this work was to quantify the variation of chamber transparency over the period of one month of measurements and its impact on estimates of peatland net ecosystem exchange. The automated transparent closed (non-steady-state) chambers are widely used for quantifying net carbon dioxide (CO_2) fluxes exchanged between different canopies and the atmosphere. However, it is known that the transparency of the chamber, and hence the amount of radiation reaching the surface, is changing over time and depends on several factors, such as solar angle, obstacles, and cleanness of the chamber surface which is exposed to the environmental conditions. The objective of this research work was to determine if the material from which the measuring chamber is made maintains constant parameters for reduction of incoming radiation in the form of photosynthetic photon flux density (PPFD) inside the chamber. Based on the obtained results, it can be stated that during the specific atmospheric conditions, the average transparency of the measuring chamber of the automatic chamber system can drop even up to 20%. If not considered, it may lead to incorrect estimation of net ecosystem exchange (NEE). In case of our experiment, non-corrected NEE flux rates were five times higher than the same fluxes after corrections. For this reason, it is important to apply correction coefficients, which allow the selection of the appropriate value for PPFD during the NEE modelling process.

1 Introduction

Due to anthropogenic activities, the climate is changing, therefore, an international agreement is reached to mitigate its impact, which gave rise to a need to understand and quantify greenhouse gas (GHG) exchange and its balances in all kinds of ecosystem, throughout the world.

Due to simple methodology of measurements and the relatively low prices of manual measuring systems, the chamber technique is most commonly applied for determining the exchange of GHGs fluxes [1,2]. This method is widely used in ecosystems like: tundra [3,4], peatlands [5–7], forests [8,9] and croplands [10,11]. Despite many advantages, this method has numerous limitations which need to be considered and minimised in order to reduce biases of estimated fluxes [1,12,13]. One of the biggest problem related to manual chamber measurements is related to their temporal resolution, which in most cases is too low [11]. That is why in order to estimate seasonal GHG balances, some models based on relationships between measured fluxes and environmental variables need to be applied [14]. One of the biggest disadvantages of manual chamber approach is that measurements are often conducted during cloudless conditions [11, 15] and that is why some site and ecosystem specific short-term events like thawing [16], precipitation [17] or sudden weather changes are often not well represented, although it is well known that they have significant impact on seasonal GHG budgets [18]. Therefore, the use of automatic chamber systems is recommended to overcome these problems. However, long-term application of transparent chambers for estimation of net CO_2 fluxes should only be possible when Photosynthetic Photon Flux Density (PPFD) sensor is installed in the chamber headspace, otherwise, due to progressive degradation of chamber transparency, the estimated fluxes may be highly uncertain. Most commonly chamber CO_2 fluxes are correlated to PPFD measured at the nearest tower or weather station [6,15]. While, it is known that any obstacles, scratches, dust or condensation of water vapour on chamber walls may lead to significant reduction of PPFD reaching the canopy surface and hence inhibit photosynthesis. Although it is not well addressed nor discussed in the literature, we assume that when CO_2 fluxes are related to PPFD taken from the nearest weather station, the estimated net and gross fluxes are often significantly overestimated. This kind of issues may be overcome when chambers are used manually, as it is relatively easy to keep the chamber clean and not shadowed. However, due to normal use and regular maintenance the surface of the transparent material is also losing its transparency. Very often, during modelling the CO_2 fluxes, the assumed reduction of PPFD in chambers is constant. For example, Chojnicki et al. [15], Minke et al. [16], and Hoffman et al. [14] assumed 95%, 88% and 84% of light transmission respectively, for chambers made from the same material of Plexiglas. Questions are however 1) if chamber transparency is really so stable overtime and we

* Corresponding author: Marcin.Strozecki@gmail.com

can use the same light transmissivity factor for all measured data independently on time and season? 2) If PPFD values taken from the nearest tower well represent the conditions inside the chamber headspace?

To answer for the above questions, we aimed to 1) determine the effect of the sun's position on the PPFD rate inside the chamber, 2) provide methods to calculate the light transmissivity correction coefficients for the transparent chamber installed in the automatic measuring system, 3) determine the impact of this light-transmissivity effect and correction factors on the rates of net ecosystem exchange (NEE).

2 Material and Methods

2.1Study site

The study site is located in the middle of the Rzecin peatland which is in the North-Western part of the Wielkopolska region in Poland (52°45'43''N 16°18'35" E, 54 m a.s.l.). The peatland vegetation is dominated by: *Sphagnum sp., Dicranum sp., Carex sp., Phragmittes com- munis, Typha langifolia, Vaccinium oxicoccus, Drosera rotundifolia, Potentilla palustris, Ranunculus acris,* and *Menyantes trifoliate* [20]. In the central part of the peatland there is a 50-70 cm thick floating peat carpet. According to FAO 2006, the peatland substrate is classified as Limnic Hemic Floatic Ombric Rheic Histosol. The annual mean air temperature is 8.5°C, while the annual precipitation sum is 526 mm. The average yearly sunshine hours are about 1547, while average annual cloudiness reaches up to 65%. The minimum occurrence of clouds is recorded in August, while the highest in December, 56% and 78%, respectively [21].

2.2 Experiment design

Chamber measurements were conducted at the WETMAN climate manipulation site located in the middle of the peatland [22]. The site consists of four treatments with three replications for each: control (C); simulated warming (W); warming and reduced precipitation (WRP); and reduced precipitation (RP). In total there are 12 plots where regular chamber measurements of CO_2 and CH_4 fluxes, but also different kind of radiation flux are carried out (details in Rastogi et al., this issue).

The automatic mobile chamber system consists of two square chambers (80 x 80 x 60 cm) made from Plexiglas and white PVC, for measurements of net CO_2 fluxes, and CO_2 and CH_4 effluxes, respectively [22]. Gas concentrations were measured with the LOSGATOS gas analyser with 1Hz frequency. The mobile platform was moving in the East-West direction and transparent chamber was not shadowed by platform construction nor by any obstacles from the south and east directions. Next to the transparent chamber, from western side, there was installed non-transparent chamber made from white PVC. Due to specific feature of our chamber system, the transparent chamber was not shadowed in the morning to early afternoon hours, but it was partly or fully shadowed by non-transparent chamber and construction of the platform in the late afternoon and evening hours, respectively. Dependently on the season, the length of the period when chamber was not shadowed was different. In order to assess the shadow effect on light transmissivity through chamber walls, the transparent chamber was equipped with PPFD radiation sensor (BF5, Delta T, USA) mounted 20 cm above the surface, inside the chamber on the north wall. As a reference, second PPFD sensor (BF5) was installed on the tower (3.5 m above surface), at 10 m distance from the experimental sites.

2.3 Data analysis

The chamber transparency experiment was carried out whole over the year in 2016, however, for the purpose of this study we present data collected for all twelve plots explicitly in June 2016. For each closure of transparent chamber, the PPFD measurement inside the chamber took 90 s and was recorded with 2 s intervals, while the reference tower-based measurements were recorded with 30 s intervals (3 values per chamber closure). In total, 991 individual measurements of incident radiation (inside and outside of the chamber), which correspond to certain CO_2 fluxes were collected in June 2016.

2.3.1 Diffusion Index, sun position and chamber transparency

Diffusion index (*DI*) was calculated as the ratio between diffused and total PPFD incident to the Earth surface (eq.1) [23]:

$$DI = \frac{PPFD_d}{PPFD_t} \text{ (-)} \quad (1)$$

where: $PPFD_d$ – Diffused Photosynthetic Photon Flux Density ($\mu mol \cdot m^{-2} \cdot s^{-1}$), $PPFD_t$ – Total Photosynthetic Photon Flux Density ($\mu mol \cdot m^{-2} \cdot s^{-1}$).

In order to characterise conditions inside the chamber headspace under cloudless, partly cloudless and cloudy conditions, three levels of DI were established: 1) ≤0.3; 2) >0.3≤0.7 and 3) >0.7, respectively. Chamber transparency was evaluated based on the ratio between the $PPFD_t$ measured inside ($PPFDt_{inside}$) and outside ($PPFDt_{outside}$) of the chamber (eq.2):

$$Transparency = \frac{PPFDt_{inside}}{PPFDt_{outside}} \times 100 \quad (2)$$

2.3.2 *CO_2 fluxes*

CO_2 fluxes (F) were calculated from the gas concentration changes in the chamber headspace ($\Delta C/\Delta t$), the chamber volume (V), and the enclosed peatland area (A) from Eq. (3):

* Corresponding author: Marcin.Strozecki@gmail.com

$$F = \frac{\Delta C}{\Delta t} \cdot \frac{V}{A \cdot M_v} \quad (3)$$

where M_v (m^3 mol^{-1}) is the molar volume of air at chamber air temperature and pressure.
The quality of calculated fluxes was evaluated in relation to coefficient of determination (R^2) of linear regression fit. All fluxes with R^2<0.8 were not considered in this study. nly fluxes measured at control plots of WETMAN site were used in this paper to calculate daily rates of net CO_2 fluxes for June 2016.

2.3.3 Modelling of Net Ecosystem Exchange

In order to determine daily rates of net ecosystem exchange (NEE) a simple rectangular, hyperbolic light response equation based on the Michaelis-Menten kinetic was applied:

$$NEE = \frac{NEE_{max} \times \alpha \times PPFD}{\alpha \times PPFD + NEE_{max}} \quad (4)$$

where: NEE is the calculated net ecosystem exchange [$\mu mol \cdot m^{-2} \cdot s^{-1}$], NEE_{max} is the maximum rate of C fixation at infinite PPFD [$\mu mol \cdot m^{-2} \cdot s^{-1}$], α is the light use efficiency [mol CO_2 mol^{-1} photons] and PPFD is the photon flux density [$\mu mol \cdot m^{-2} \cdot s^{-1}$].

Monthly-specific α and NEE_{max} parameters were estimated based on the measured NEE and PPFD values for each plot independently. They were used to calculate NEE fluxes based on PPFD measured at the tower and plot-specific PPFD correction factors, with 30-minutes time steps. Average daily NEE was calculate for periods between sunrise to sunset, when PPFD exceeds 50 $\mu mol \cdot m^{-2} \cdot s^{-1}$.

2.3.4 PPFD correction factors

Due to observed differences in PPFD measured inside and outside of the chamber, the plot-specific PPFD correction factors were calculated in order to correct (reduce) the tower-based PPFD used for the modelling of net CO_2 fluxes. The calculations were made for datasets representing early morning to early afternoon hours (1) and late afternoon to early evening hours (2) and different DIs levels: 1) <0.3, 2) 0.3-0.7 and 3) >0.7. The analyses were made in R ver. 3.4.3 based on correlation plots (1:1) where inside and outside PPFD rates were plotted against each other.

2.3.5 Statistical analyses

The normal distribution of the collected data was analyzed by means of the Shapiro - Wilk test. Since the data pass the normality test, then the Student's t-test was applied to determine the similarity of the analyzed data. All statistical tests were performed with R software version 3.1.2 using the xts, plyr, doBy, nortest packages.

3 Results and Discussion

3.1 Transparency of the chamber

The Sun position during the day was calculated by means of the online open-source R package 'suncalc' for the exact location of the WETMAN experiment and the time when radiation (PPFD) measurements were taken in the transparent chamber. Dependently on the solar azimuth and time of the day the chamber transparency varied from 20% to 95% (Fig.1) revealing the very clear daily variations of the light transmissivity through chamber walls. The lowest transparency of the chamber was recorded at the lowest PPFD and the lowest positions of the sun in the morning and evening hours. However, in the late afternoon when the sun azimuth exceeded 250° the chamber transparency reached the lowest daily values of 20%, mainly due to shadowing of the chamber by the platform and non-transparent chamber.

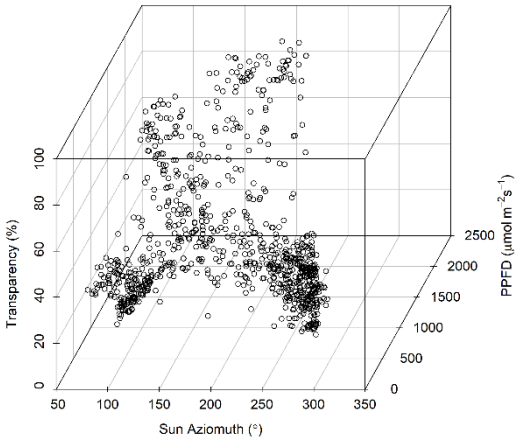

Fig.1. Dependence of the chamber transparency (%) on azimuth of the Sun and PPFD in June 2016 (n=991).

For the purpose of data visualisation and assessment of the effect of time and solar azimuth on chamber transparency, two groups of data were separated: 1) data measured from sunrise when PPFD exceeded 50 $\mu mol \cdot m^{-2} \cdot s^{-1}$ till 1:00 pm, when we are sure that the radiation sensor in the transparent chamber was not shadowed by chamber system and 2) all daily data collected after 1:00 pm till sunset when PPFD decreased below 50 $\mu mol \cdot m^{-2} \cdot s^{-1}$, when chamber was partly or fully shadowed (Fig. 2). Monthly daily mean PPFD rates inside and outside of the chamber in June 2016 reached 740 $\mu mol \cdot m^{-2} \cdot s^{-1}$ and 1180 $\mu mol \cdot m^{-2} \cdot s^{-1}$, respectively and they were significantly different ($p<2.2*10^{-16}$). However, one must bear in mind that the ratio between PPFD recorded inside and outside of the chamber is changing proportionally to the DI factor (Fig. 2).

* Corresponding author: Marcin.Strozecki@gmail.com

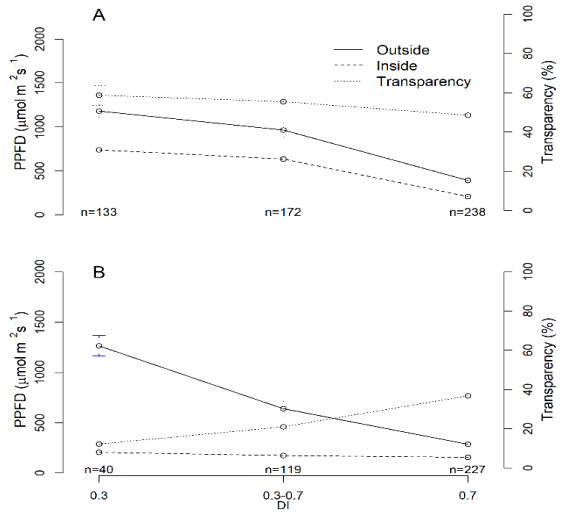

Fig. 2. Monthly daily means of PPFD (µmol·m^{-2}·s^{-1}) in June 2016, for DI 1) <0.3, 2) 0.3-0.7 and 3) >0.7; and for different time of measurements: A) from sunrise till 1:00 pm; and B) from 1:00 pm till sunset (details in the text).

The average monthly transparency of the chamber varied from around 60% to 50% for the dataset collected in the morning and early afternoon hours and from around 20% to 40% in the afternoon and evening hours, for DI<0.3 and DI>0.7, respectively (p=0.0001916). The highest values of chamber transparency exceeding 60% in average were recorded during sunny days (DI <0.3) and for the first part of the day (from 6:00 am to 1:00 pm). For this dataset, chamber transparency decreased slightly with increasing DI (Fig. 2A), and the differences were significant (p<0.0189). Surprisingly, for the afternoon dataset the transparency of the chamber was reversely related to DI and it reached the highest values of about 40% at DI>0.7. These results indicate the effect of diffused radiation which comes to the plot surface from different directions independently on the sun position. On the other hand, this effect indicates that in the afternoon hours and during sunny conditions our PPFD sensor in the transparent chamber and chamber itself are significantly shadowed and the amount of radiation reaching the surface is significantly smaller than on non-shadowed plots. Although differences between transparency of the chamber at the DI>0.7 for both groups of datasets presented in fig. 2 are not significant, the differences between chamber transparency for DI between 0.3 and 0.7 as well as <0.3 are increasing with decreasing DI and they are significant (p<0.05).

2.2 PPFD correction factors to determine rates of light transmission through the chamber walls

Based on the PPFD values measured inside and outside of the chamber, the PPFD correction factors were calculated (Fig. 3). They were estimated for each of the 12 plots independently, for three levels of DI and for two datasets: A) from sunrise till 1:00 pm; and B) from 1:00 pm till sunset. The PPFD correction factors (fPPFD) varied from 0.48 till 0.97.

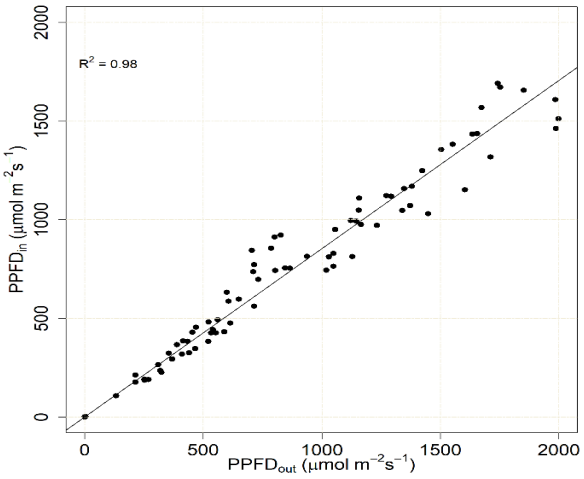

Fig. 3. Correlation plot showing the example of regressions between inside and outside PPFD for DI<0.3 and data representing early morning till early afternoon hours.

The smallest monthly averages of fPPFD (0.57±0.08) for the A dataset were calculated for DI between 0.3 and 0.7, while for B dataset the smallest fPPFD (0.64±0.11) were estimated in case of data recorded over the sunny conditions (DI<0.3). For the A dataset the monthly average fPPFD were around 0.82 for data collected at sunny (DI<0.3) and cloudy (DI>0.7) conditions. Whereas, for B dataset the values of average monthly fPPFD increased with increasing participation of diffused radiation, and the highest value of 0.97±0.01 were calculated for the DI>0.7.

Table 1. Summarised PPFD correction factors for twelve measuring plots.

plots	DI between sunrise till 1:00 pm			DI between 1:00 pm till sunset		
	<0.3	0.3 - 0.7	>0.7	<0.3	0.3 - 0.7	>0.7
1	0.76	0.67	0.84	0.82	0.77	0.97
2	0.95	0.66	0.82	0.77	0.79	0.97
3	0.82	0.65	0.84	0.66	0.69	0.96
4	0.77	0.62	0.75	0.54	0.92	0.97
5	0.75	0.58	0.79	0.62	0.85	0.97
6	0.80	0.48	0.87	0.76	0.83	0.97
7	0.90	0.46	0.82	0.42	0.77	0.95
8	0.89	0.50	0.79	0.52	0.77	0.97
9	0.83	0.48	0.81	0.64	0.81	0.96
10	0.79	0.55	0.80	0.61	0.78	0.97
11	0.88	0.63	0.87	0.69	0.79	0.96
12	0.78	0.58	0.83	0.70	0.78	0.96
average ±SD	0.83 ± 0.06	0.57 ± 0.08	0.82 ± 0.03	0.64 ± 0.11	0.80 ± 0.05	0.97 ± 0.01

* Corresponding author: Marcin.Strozecki@gmail.com

2.3 Impact of PPFD correction factors on modelled NEE

As shown in Figure 4, diurnal cycles of the modelled NEE rates for the exemplary cloudless day of June 2016 are significantly different (p = 0.0147) for the conditions with and without corrections of PPFD. It can be noticed that the difference in modelled NEE increases over time till around 9 am and then in around solar-noon hours (from 9 am to 4 pm) the difference is rather stable and starts to decrease after 4 pm. It is strongly correlated with the sun position over the horizon and amount of PPFD reaching the peatland surface (Fig. 5).

Of course the question may arise here which fluxes are real, or which one are closer to reality. As we cannot use other experimental data to verify our hypothesis we can only speculate that fluxes modelled based on the tower-based PPFD measurements are significantly overestimated (which is confirmed by data shown in Fig. 4) because lower CO_2 fluxes measured at the conditions when photosynthesis is reduced due to lower PPFD reaching the canopy surface are correlated with higher PPFD values, which do not correspond to the conditions inside the chamber.

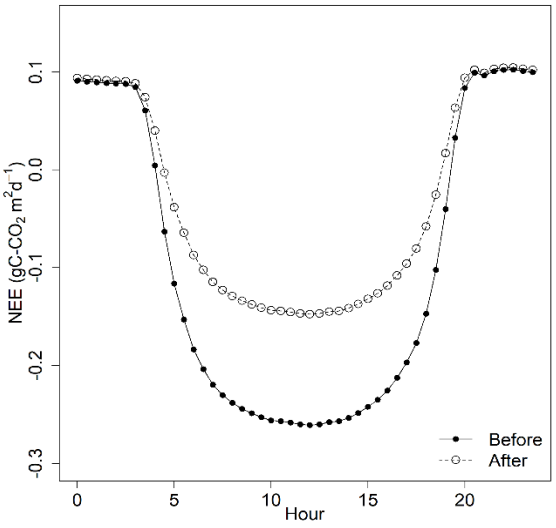

Fig. 4. Modelled diurnal courses of the net ecosystem CO_2 fluxes before and after PPFD correction.

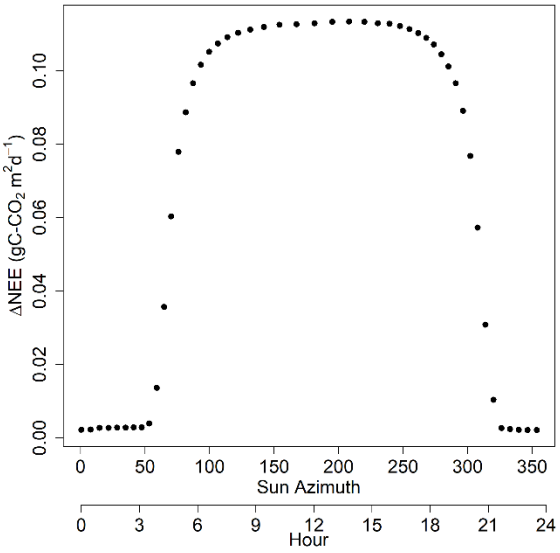

Fig. 5. Relationship between ΔNEE and solar azimuth for exemplary cloudless day presented in Fig. 4.

This means, for the entire analysed period of June 2016 the average daily NEE flux rates calculated based on the non-corrected PPFD will be around -3.8 gC-CO_2 m^2 d^{-1}, while when the PPFD corrections are applied the same average daily NEE will reach -0.7 gC-CO_2 m^2 d^{-1} (Fig. 6), and this difference is statistically significant ($p<0.05$). It has to be noticed here, that negative net CO_2 fluxes denote that uptake of CO_2 in photosynthesis exceeds CO_2 emission through autotrophic and heterotrophic respiration [6,15]. The monthly cumulative NEE (NEE_{June}) calculated based on these two datasets are also significantly different ($p<0.05$). If not corrected, NEE_{June} exceeds -342 gCO_2-C m^{-2} while after corrections it does not exceed -64 gCO_2-C m^{-2}.

Comparison of these two datasets shows how important is to consider the diurnal changes in transparency of the NEE chamber in determination of the daily and seasonal flux rates. Many researchers assume that the chamber transparency does not change over time and is stable for the entire season [15,19]. However, our results indicate that if this PPFD correction is not applied, or is applied incorrectly, the calculated NEE fluxes are significantly overestimated. In case of our experiment, non-corrected NEE flux rates were five times higher than the same fluxes after corrections.

* Corresponding author: Marcin.Strozecki@gmail.com

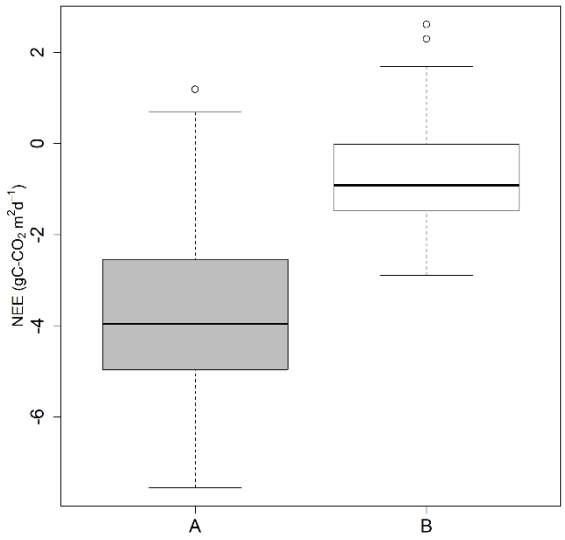

Fig. 6. Comparison of the modelled average daily NEE fluxes for June 2016. "A" represent NEE fluxes before PPFD correction and "B" – NEE after PPFD correction.

Conclusion

Transparency of the NEE chamber is not stable over time and is changing dependently on the solar azimuth and hence time of the day. The light transmission through the chamber walls is the highest in around solar-noon hours and the smallest in the morning and evening hours. This effect should be considered during the CO_2 flux modelling and PPFD correction factors shall be applied in order to well represent the radiation conditions inside the transparent chambers. In order to calculate these radiation correction factors, transparent chamber need to be equipped with radiation sensors of the same type as on the nearest tower. Modelling of NEE fluxes based on non-corrected PPFD may lead to significant overestimation of the fluxes and hence make the seasonal CO_2 balances highly uncertain.

Acknowledgement

The Research was co-founded by the National Science Centre of Poland within the **OPUS project:** ***Sun Induced florescence and photosynthesis of peatland vegetation response to stress caused by water deficits and increased temperature under conditions of climate manipulation experiment*** **(No. 72016/21/B/ST10/02271)** and the Polish National Centre for Research and Development within the Polish-Norwegian Research Programme within the **WETMAN project (C*entral European Wetland Ecosystem Feedbacks to Changing Climate – Field Scale Manipulation,* Pol-Nor/203258/31/2013**. Authors would like to thank all the WETMAN team members who worked on the station and helped to develop and maintain the WETMAN site climate manipulation infrastructure, especially to Janusz Olejnik, Jacek Leśny, Marek Urbaniak, Bogdan Chojnicki, Damian Józefczyk, Mateusz Samson, Mariusz Lamentowicz, Dominika Łuców, Anna Basińska, Monika Reczuga.

References

1. L. Kutzbach, J. Schneider, T. Sachs, M. Giebels, H. Nykanen, N. J. Shurpali, P. J. Martikainen, J. Alm, M. Wilmking, Biogeosciences **4**, 1005 (2007)
2. G. Wohlfahrt, Ch. Anfang, M. Bahn, A. Haslwanter, Ch. Newesely, M. Schmitt, M. Drösler, J. Pfadenhauer, A. Cernusca, Agric. For. Meteorol. **128**, 141 (2005)
3. G. Celis, M. Mauritz, R. Bracho, V. G. Salmon, E.E. Webb, J. Hutchings, S.M. Natali, C. Schädel, K.G. Crummer, E.A.G. Schuur, J. Geophys. Res. Biogeosci. **122**, 1471 (2017)
4. S. M. Natali, E. Schuur, M. Mauritz, J. Schade, G. Celis, K. Crummer, C. Johnson, J. Krapek, E. Pegoraro, V. Salmon, E. Webb, J. Geophys. Res. Biogeosci. **120**, 525 (2015)
5. R. Juszczak, J. Augustin Wetlands **33**, 895 (2013)
6. M. Acosta, R. Juszczak, B. Chojnicki, M. Pavelka, K. Havránková, J. Leśny J., L. Krupková L., M. Urbaniak, K. Machačová, J. Olejnik, Wetlands **37**, 3 (2017)
7. M. Samson, S. Słowińska, M. Słowiński, M. Lamentowicz, J. Barabach, K. Harenda, M. Zielińska, B.J.M. Robroek, V.E.J. Jassey, A. Buttler, B.H. Chojnicki, Wetlands **38**, 551 (2018)
8. J.A. Subke, J.D. Tenhunen, Agri. Forest Meteorol. **126**, 157 (2004)
9. P. Kolari, J. Pumpannen, L. Kulmala, H. Ilvesniemi, E. Nikinmaa, T.Grönholm, P. Hari, Forest Ecology and Management **221**, 241 (2006)
10. M. Hoffmann, S. J. Wirth, H. Beßler, C. Engels, H. Jochheim, M. Sommer, J. Augustin, Nutr. Soil Sci. **181**, 41 (2018)
11. B. Uździcka, M. Stróżecki, M. Urbaniak, R. Juszczak, International Agrophysics **31**, 419 (2017)
12. R. Juszczak, Int. Agrophys. **27**, 159 (2013)
13. J.R. Christiansen, J. Korhonen, R. Juszczak, M. Giebels, M. Pihlatie, Plant and Soil **343**, 171 (2011)
14. M. Hoffmann, N. Jurisch, E. Albiac Borraz, U. Hagemann, M. Drösler, M. Sommer, J. Augustin, Agric. For. Meteorol. **200**, 30 (2015)
15. B.H. Chojnicki, M. Michalak, M. Acosta, R. Juszczak, J. Augustin, M. Drösler, J. Olejnik, Polish J. Environ. Stud. **19**, 283 (2010)
16. J. Bubier, P. Crill and A. Mosedale, Hydrol. Process. **16**, 3667 (2002)
17. C. Wayson, J. Randolph, P. Hanson, C.S.B Grimmond, H.P. Shmid, Biogeochemistry **80**, 173 (2006)
18. N.S. Panikov, S.N. Dedysh. Global Biogeochemical Cycles **14**, 1071 (2000)

* Corresponding author: Marcin.Strozecki@gmail.com

19. M. Minke, J. Augustin, A. Burlo, T. Yarmashuk, H. Chuvashova, A. Thiele, A Freibauer, V. Tikhonov, M. Hoffman. Biogeosciences **13**, 3945 (2016)
20. M. Lamentowicz, M. Mueller, M. Gałka, J. Barabach, K. Milecka, T. Goslar, M. Binkowski, Quaternary International **357**, 282 (2015)
21. A. Woś, *The climate of Poland* (in Polish; original title: *Klimat Polski*) (Wydawnictwo Naukowe PWN, Warszawa, 1999)
22. R. Juszczak, A. Basinska, B. Chojnicki, M. Gabka, M. Hoffmann, D. Józefczyk, M. Lamentowicz, J. Leśny, D. Luców, C. Moni, M. Reczuga, M. Samson, H. Silvennoinen, M. Strózecki, M. Urbaniak, M. Zielinska, J. Olejnik, Geophysical Research Abstracts **19**, EGU2017-18838-1 (2017)
23. O. Urban, K. Klem, A. Ač, K. Havránková, P. Holišová, M. Navrátil, J. Grace, Funct. Ecol. **26**, 46 (2012)

* Corresponding author: Marcin.Strozecki@gmail.com